Applied Physics Letters ARTICLE scitation.org/journal/apl

Epitaxial lift-off CdTe/MgCdTe double heterostructures for thin-film and flexible solar cells applications

Cite as: Appl. Phys. Lett. **118**, 181101 (2021); doi: 10.1063/5.0049377
Submitted: 4 March 2021 · Accepted: 3 April 2021 ·
Published Online: 3 May 2021

View Online Export Citation CrossMark

Jia Ding,[1,2] Cheng-Ying Tsai,[1,2] Zheng Ju,[1,3] and Yong-Hang Zhang[1,2,a)]

AFFILIATIONS

[1]Center for Photonics Innovation, Arizona State University, Tempe, Arizona 85287, USA
[2]School of Electrical, Computer and Energy Engineering, Arizona State University, Tempe, Arizona 85287, USA
[3]Department of Physics, Arizona State University, Tempe, Arizona 85287, USA

[a)]**Author to whom correspondence should be addressed:** yhzhang@asu.edu

ABSTRACT

This paper reports an improved epitaxial lift-off (ELO) technology for monocrystalline CdTe/MgCdTe double-heterostructure (DH) thin films using water-soluble and nearly lattice-matched MgTe as a sacrificial layer. Employing hard-baked photoresist as the superstrates with appropriate surface tension, the lift-off thin films show smooth and flat surfaces, confirmed by atomic-force microscopy profiles. Photoluminescence (PL) measurements reveal further enhancement of the light extraction from the ELO thin films with a coated Ag back reflective mirror. The increased PL intensity also confirms that the CdTe/MgCdTe DHs maintain high optical quality after ELO. External luminescence quantum efficiency (η_{ext}) is quantitatively measured and used to calculate the implied open-circuit voltage (iV_{OC}). A 0.5-μm-thick lift-off CdTe/MgCdTe DH with a back mirror demonstrates an η_{ext} value of 5.35% and an iV_{OC} value of 1.152 V. The devices based on this structure are also expected to have an improved fill factor and a short-circuit current density (J_{SC}) of 24.7 mA/cm^2 according to the simulation results, promising to achieve CdTe solar cells with a record power conversion efficiency.

Flexible thin-film solar cells with a high power density and specific power are highly desirable for both terrestrial and space applications. Epitaxial lift-off (ELO) technology, which enables the development of flexible thin-film solar cells, has been successfully demonstrated for III–V materials and ZnSe-based II–VI semiconductors[1–3] using highly selective etchants and sacrificial layers. For the ELO applications to thin film photovoltaics, like polycrystalline CdTe and $CuIn_xGa_{1-x}Se_2$ (CIGS) solar cells, following the sacrificial layer approach, devices were made on polyimide films by constructing a glass/NaCl/polyimide/CdTe (CIGS) stack and then dissolving NaCl in water.[4,5] Another ELO method was demonstrated by depositing polycrystalline CdS/CdTe films on the Si/SiO_2 substrate, showing a fast lift-off process in water.[6] Although the thin films can be delaminated automatically, these methods are limited to polycrystalline systems due to the large lattice mismatch between substrates or sacrificial layers and the epitaxial thin films. Besides the sacrificial layer approach, several mechanical or thermomechanical lift-off methods were reported, such as delaminating CIGS films on an Mo layer and lifting-off CdTe films with a controlled stressor of polymeric handled in liquid nitrogen.[7–9] Although these methods demonstrated novel approaches to delaminate high-quality polycrystalline thin films, there is no report on the ELO process of high-quality monocrystalline CdTe devices.

Recently, a new ELO method for monocrystalline CdTe thin films was reported using MgTe as a sacrificial layer.[10–12] High-quality CdTe/MgCdTe double heterostructure (DH) and MgTe can be grown on a nearly lattice-matched InSb substrate by using molecular-beam epitaxy (MBE). The sacrificial layer, MgTe, is water-soluble, while both the DH and the substrate have extremely low etching rates in deionized (DI) water. Therefore, this ELO method is promising to obtain high-quality monocrystalline DH thin films. Since only water is used during the ELO process, the substrate is intact and can be reused almost indefinitely, without the need for repolishing. Furthermore, the wide-bandgap MgCdTe barriers serve as carrier selective barriers and passivation layers to the CdTe absorber. Therefore, the lift-off MgCdTe surface is expected to have little impact on the effective minority carrier lifetime of the CdTe DH.[13] To enhance the light extraction and photon-recycling effect, a back reflective mirror can be added. With a back mirror, the necessary absorber thickness can be reduced to approximately half of the original value, leading to decreased total SRH recombination current density, increased open-circuit voltage (V_{OC}), and nearly the same short-circuit current density (J_{SC}). A similar approach has been successfully used to demonstrate thin-film GaAs solar cells with a record efficiency of 29.1%.[14] For the previous study of MgTe-based ELO,[12] Kapton tape was used as the superstrate, attached to the top surface of the sample. By submerging the sample in DI water, the thin film was lifted off with the tape. Although the process was successful, the Kapton tape is not an ideal superstrate since the tape makes the thin film develop wrinkles and defects during the ELO process, thus giving much lower photoluminescence (PL) intensity in the center area and broadened CdTe peak in the x-ray diffraction (XRD) pattern. The strong PL signals observed at the lift-off thin film edges are attributed to the luminescence concentration as the film acts as an efficient waveguide. In this work, hard-baked photoresist is used as a superstrate to supply more rigid support to the thin film during the ELO process, as well as needed surface tension that enables the reaction products of the thin MgTe with DI water to diffuse out from the etching fronts and let the etching continue.

The basic process of MgTe-based ELO conducted in this study is depicted in Fig. 1. Upon removal from the MBE chamber, each sample is coated with photoresist and then moved to a hot plate for hard bake. Several layers of photoresist are coated to achieve an appropriate amount of tension. The sample is then immersed in DI water. MgTe is dissociated, and the CdTe thin film with photoresist is lifted off. Typically, the process takes about 15 min to lift off a 1 cm × 1 cm thin film from the substrate in 55 °C DI water. The free-standing thin film is then transferred to a foreign substrate, a polyethylene terephthalate (PET) coated with Ag as a reflective mirror. To fabricate thin-film solar cells in the future, it is planned to use indium to bond the CdTe lift-off samples with conductive PET substrates before the lift-off process,[15] or to use an elastomer, like PDMS, as the superstrate to lift off, transfer, and print the thin films.[16,17]

Figure 2(a) shows the layer structure of a conventional CdTe/MgCdTe DH solar cell design, which exhibits a record V_{OC} value up to 1.11 V.[18,19] The CdTe lift-off samples in this study, which are shown in Fig. 2(b), are designed with a reversed layer sequence to be compatible with the ELO process mentioned above. Except for the layer sequence, the changes in the new designs are (i) the thickness of the i-$Mg_{0.4}Cd_{0.6}Te$ barrier was increased from 15 to 20 nm to minimize electron tunneling and consequent p-contact/i-$Mg_{0.4}Cd_{0.6}Te$ interface recombination,[20,21] (ii) the thickness of the n-$Mg_{0.24}Cd_{0.76}Te$ barrier was decreased from 50 nm to 20 nm to reduce the parasitic absorption considering the light reflection from the back mirror, and (iii) two structures A and B feature the different absorber thickness of 0.5 and 1 μm, respectively.

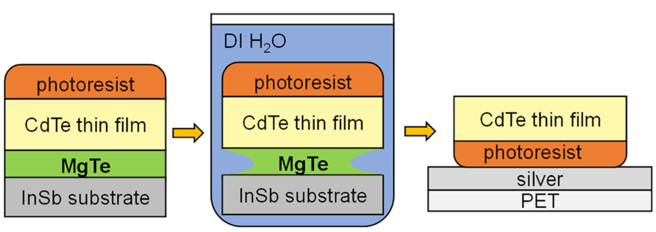

FIG. 1. Schematic ELO process of CdTe/MgCdTe DH, using photoresist as the superstrate.

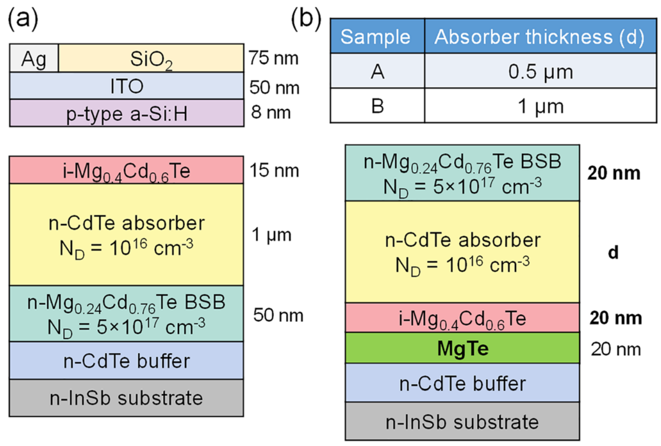

FIG. 2. (a) Layer structure of the conventional CdTe/MgCdTe DH solar cell design. (b) Layer structures of newly designed CdTe lift-off samples with MgTe sacrificial layers.

To illustrate the crystalline properties of the lift-off thin films and the successful ELO process, (004) ω-2θ XRD scans of structure A both pre-ELO (top) and post-ELO (bottom) are shown in Fig. 3. Compared to the pre-ELO scan, the post-ELO scan shows that both the MgTe peak at 29° and the InSb substrate peak are absent, while the CdTe absorber peak and the features corresponding to the $Mg_{0.24}Cd_{0.76}Te$ and $Mg_{0.4}Cd_{0.6}Te$ barriers remain. The full width at half maximum (FWHM) of the CdTe absorber peak does not change significantly

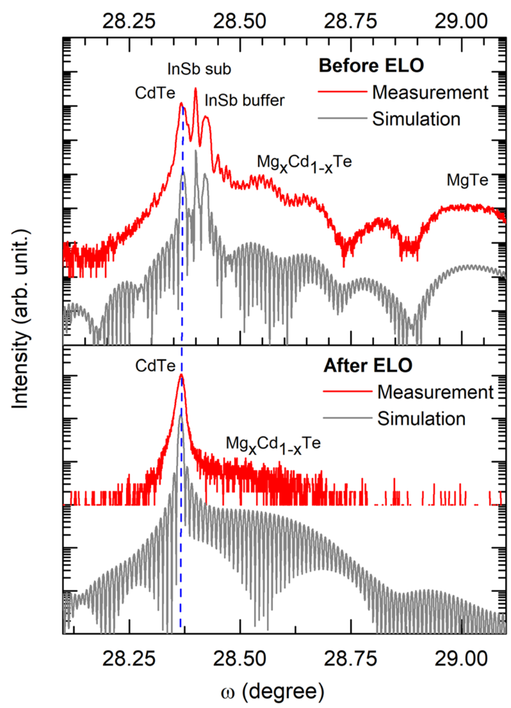

FIG. 3. Omega-2θ (004) scans of (top) as-grown sample A on an InSb(001) substrate and (bottom) the free-standing CdTe/MgCdTe DH thin film after ELO.

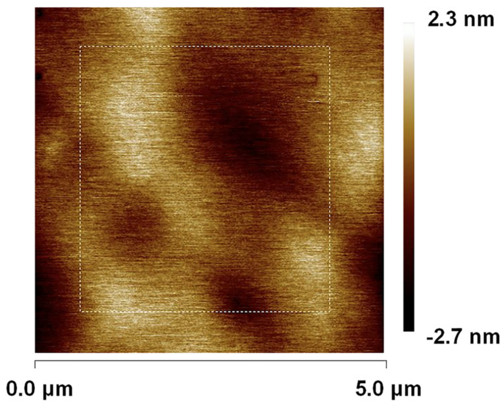

FIG. 4. AFM image of i-$Mg_{0.4}Cd_{0.6}Te$ surface morphology of the post-ELO thin film with structure B in the $5 \times 5\,\mu m^2$ range.

after the ELO. These findings indicate a successful ELO of the CdTe DH thin films with the assistance of photoresist.

After the ELO, the i-$Mg_{0.4}Cd_{0.6}Te$ layer, which passivates the CdTe absorber and serves as an electron blocking layer, is exposed to the air. If this layer reacts with DI water due to the 40% composition of Mg in MgCdTe during the ELO process, the enhanced surface recombination would lead to low optical performance of the thin film although the crystalline quality remains unchanged.[20,22] To confirm the DH, especially that the i-$Mg_{0.4}Cd_{0.6}Te$ layer is intact after the ELO, the i-$Mg_{0.4}Cd_{0.6}Te$ surface morphology of the post-ELO thin film with structure B is characterized by atomic-force microscopy (AFM). A $5\,\mu m \times 5\,\mu m$ range image is shown in Fig. 4, with a root mean square (RMS) roughness of 6.69 Å, similar to that obtained on an epitaxial layer surface, suggesting the extremely low etching rate of i-$Mg_{0.4}Cd_{0.6}Te$ in DI water.

The optical performance of the as-grown samples and post-ELO thin films is first characterized by using room-temperature PL spectroscopy. The laser wavelength is 532 nm, with a penetration depth in the CdTe absorber smaller than $0.1\,\mu m$. Figure 5(a) compares the PL of a conventional CdTe DH sample and the lift-off samples with structures A and B before ELO. Compared with the conventional CdTe DH sample, the lift-off samples give stronger PL signals because the thicker i-$Mg_{0.4}Cd_{0.6}Te$ barrier further suppresses the tunneling of the photogenerated carriers from the absorber to the surface to recombine non-radiatively.[20,21] With a thinner absorber, the lift-off sample with structure A shows even higher PL intensity than structure B due to a higher photon-generated carrier density per unit volume and lower total SRH non-radiative recombination rate per unit area. In Fig. 5(b), stronger PL intensities in the post-ELO films than those in the as-grown lift-off samples are observed. This shows that the light extraction and photon-recycling effect of the CdTe thin films have been enhanced by replacing the absorptive substrate with a reflective back mirror. Increased PL intensity is observed across the sample areas of the post-ELO films.

In addition to PL spectra, photoluminescence quantum efficiency (PLQE) measurements are performed, and external luminescence quantum efficiency (η_{ext}) is quantitatively measured. More details about the experimental procedures and theoretical analysis can be found in Ref. 23. Through the following formula:[24,25]

$$iV_{OC} = V_{OC,ideal} - \frac{kT}{q}\left|\ln(\eta_{ext})\right|,$$

the implied open-circuit voltage (iV_{OC}) of a solar cell, or the quasi-fermi-level splitting in the absorber region, can be measured, where η_{ext} is the ratio of photons that escape from the front surface to the electron-hole pairs generated in the solar cell absorber; $V_{OC,ideal}$ is the V_{OC} of a solar cell when the recombination is purely radiative, emittance to the back surface is zero, and zero voltage loss is due to carrier transport. The results are summarized in Table I.

One of the key factors to make a precise calculation of iV_{OC} is the accurate estimation of light absorption, i.e., the number of carriers optically injected into the CdTe absorber. Different structures with different smooth/textured surfaces, absorptive/reflective substrates, and

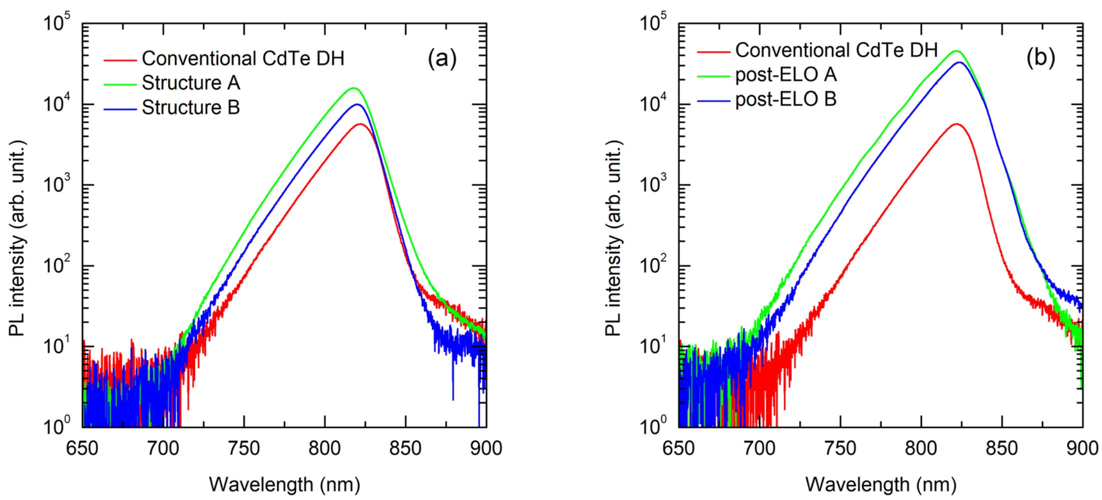

FIG. 5. (a) Comparison of the PL spectra between the conventional CdTe DH sample and as-grown CdTe lift-off samples with structures A and B. (b) Comparison between the conventional CdTe DH sample and free-standing thin films of structures A and B with Ag back mirror.

TABLE I. Summary of PLQE measurement results. SC design represents conventional monocrystalline CdTe DH solar cell design.

Sample	η_{ext} at 1 sun	iV_{OC} (V)	V_{OC} (V)
SC design	1.54%	1.119	1.11[19]
Structure A	3.65%	1.141	…
Structure B	1.80%	1.123	…
ELO A	5.35%	1.152	
ELO B	3.39%	1.139	

reflective index, etc., would have different absorption. A total of 12 kinds of statistical ray tracing models are presented in the previous studies,[26,27] assuming the maximal scattering case with an angular Lambertian distribution. For the MBE grown samples and post-ELO thin films with smooth surfaces and interfaces, the absorption of the CdTe absorber at the laser wavelength can be accurately simulated by wave optics, taking into account of the optical constants (refractive index, n, and extinction coefficient, k) and the thickness of each layer. One example is that the measured iV_{OC} of the conventional CdTe DH samples was in excellent agreement with V_{OC} of the processed solar cells.[19] In the light absorption simulation of the above ELO thin films, however, the absorption of photoresist is ignored. Therefore, the calculated iV_{OC} values of the ELO films are underestimated. Based on the measurements, ELO thin films with a 0.5-μm-thick absorber (ELO A) demonstrated an η_{ext} value of 5.35% and an iV_{OC} value of 1.152 V. Using the same processing flow of the conventional CdTe DH solar cells, the CdTe thin-film solar cells based on structure A would achieve a V_{OC} value of 1.15 V or even higher.

Compared with the conventional CdTe DH solar cell design, a thin-film solar cell with a 0.5-μm-thick absorber would maintain a similar J_{SC} by incorporating a 150-nm-thick Ag layer as back mirror.

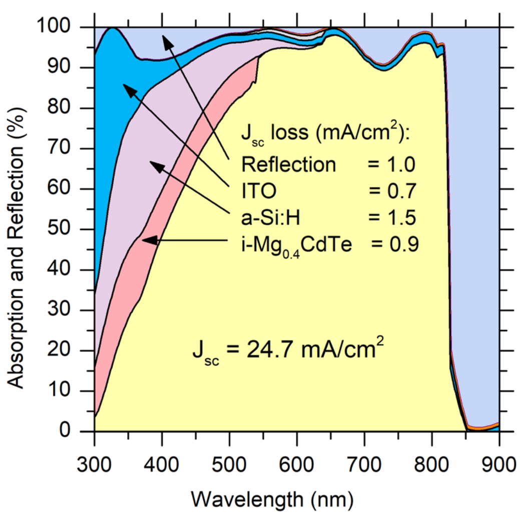

FIG. 6. Simulated absorptance spectrum for CdTe thin-film solar cells with a calculated photo-current density of 24.7 mA/cm^2. The simulated device (structure A) has a 75-nm-thick SiO_2 anti-reflection coating layer, a 55-nm-thick ITO layer, an 8-nm-thick a-Si:H hole-contact layer, and a 150-nm-thick Ag back contact.

The simulated structure is SiO_2/ITO/a-Si:H/CdTe DH (structure A)/Ag/PET. Figure 6 depicts the simulated absorption of the thin-film solar cells with a calculated photo-current density of 24.7 mA/cm^2 using wave optics. By optimizing the p-contact to reduce the parasitic absorption, such as depositing a thinner a-Si:H layer with higher doping density or replacing the a-Si:H with a wider-bandgap material, the J_{SC} of thin-film solar cells can be further improved.

In summary, this paper demonstrates a photoresist-assisted ELO method to obtain high-quality monocrystalline CdTe DH thin films with a smooth lift-off surface and enhanced optical performance. A maximum η_{ext} value of 5.35% is extracted from a newly designed, 0.5-μm-thick CdTe/MgCdTe DH after the ELO process, corresponding to an iV_{OC} value of 1.152 V, which is only 0.35 V below the bandgap of monocrystalline CdTe. By incorporating the back reflective mirror to increase the optical thickness and photo-recycling effect, the J_{SC} value of a processed 0.5-μm-thick CdTe thin-film solar cell is 24.7 mA/cm^2 according to simulation.

This work was partially supported by AFRL (Grant No. FA9453-20-2-0011). The authors acknowledge Allison McMinn for proofreading the manuscript and suggestions and the LeRoy Eyring Center for Solid State Science at Arizona State University for the use of facilities.

DATA AVAILABILITY

The data that support the findings of this study are available from the corresponding author upon reasonable request.

REFERENCES

[1]M. Konagai, M. Sugimoto, and K. Takahashi, J. Cryst. Growth **45**, 277 (1978).
[2]E. Yablonovitch, T. Gmitter, J. P. Harbison, and R. Bhat, Appl. Phys. Lett. **51**, 2222 (1987).
[3]A. Balocchi, A. Curran, T. C. M. Graham, C. Bradford, K. A. Prior, and R. J. Warburton, Appl. Phys. Lett. **86**, 011915 (2005).
[4]A. N. Tiwari, A. Romeo, D. Baetzner, and H. Zogg, Prog. Photovoltaics Res. Appl. **9**, 211 (2001).
[5]A. N. Tiwari, M. Krejci, F.-J. Haug, and H. Zogg, Prog. Photovoltaics Res. Appl. **7**, 393–397 (1999).
[6]D. J. Magginetti, J. A. Aguiar, J. R. Winger, M. A. Scarpulla, E. Pourshaban, and H. P. Yoon, Adv. Mater. Interfaces **6**, 1900300 (2019).
[7]D. F. Marron, A. Meeder, S. Sadewasser, R. Wurz, C. A. Kaufmann, T. Glatzel, T. Schedel-Niedrig, and M. C. Lux-Steiner, J. Appl. Phys. **97**, 094915 (2005).
[8]D. L. McGott, M. D. Kempe, S. Glynn, N. Bosco, T. M. Barnes, N. M. Haegel, C. A. Wolden, and M. O. Reese, ACS Appl. Mater. Interfaces **10**, 44854 (2018).
[9]S. M. Jovanovic, G. A. Devenyi, P. Kuyanov, J. L. Carvalho, K. Meinander, R. R. LaPierre, and J. S. Preston, Mater. Res. Express **6**, 025913 (2018).
[10]B. Seredyński, M. Król, P. Starzyk, R. Mirek, M. Ściesiek, K. Sobczak, J. Borysiuk, D. Stephan, J.-G. Rousset, J. Szczytko, B. Piętka, and W. Pacuski, Phys. Rev. Mater. **2**, 043406 (2018).
[11]C. M. Campbell, C.-Y. Tsai, J. Ding, T. T. McCarthy, B. Seredyński, W. Pacuski, and Y.-H. Zhang, in 45th IEEE Photovoltaics Special Conference (Oral Presentation), Hawaii, 10–15 June 2018.
[12]C. M. Campbell, C.-Y. Tsai, J. Ding, and Y.-H. Zhang, IEEE J. Photovoltaics **9**, 1834–1838 (2019).
[13]S. Liu, X.-H. Zhao, C. M. Campbell, M. B. Lassise, Y. Zhao, and Y.-H. Zhang, Appl. Phys. Lett. **107**, 041120 (2015).
[14]M. A. Green, Prog. Photovoltaics: Res. Appl. **20**, 472–476 (2012).
[15]W. Yang, J. Becker, S. Liu, Y.-S. Kuo, J.-J. Li, B. Landini, K. Campman, and Y.-H. Zhang, J. Appl. Phys. **115**, 203105 (2014).
[16]W. Yang, H. Yang, G. Qin, Z. Ma, J. Berggren, M. Hammar, R. Soref, and W. Zhou, Appl. Phys. Lett. **96**, 121107 (2010).

[17] S. J. Cho, D. Liu, J.-H. Seo, R. Dalmau, K. Kim, J. Park, J. Gong, D. Zhao, F. Wang, X. Yin, Y. H. Jung, I.-K. Lee, M. Kim, X. Wang, J. D. Albrecht, W. Zhou, B. Moody, and Z. Ma, New J. Phys. **21**, 023011 (2019).
[18] Y. Zhao, M. Boccard, S. Liu, J. Becker, X.-H. Zhao, C. M. Campbell, E. Suarez, M. B. Lassise, Z. Holman, and Y.-H. Zhang, Nat. Energy **1**, 16067 (2016).
[19] J. J. Becker, M. Boccard, C. M. Campbell, Y. Zhao, M. Lassise, Z. C. Holman, and Y.-H. Zhang, IEEE J. Photovoltaics **7**, 900–905 (2017).
[20] X.-H. Zhao, S. Liu, C. M. Campbell, Y. Zhao, M. B. Lassise, and Y.-H. Zhang, IEEE J. Photovoltaics **7**, 913–918 (2017).
[21] J. Ding and Y.-H. Zhang, in Proceedings of the 46th IEEE Photovoltaics Special Conference, Chicago, 16–21 June (2019), pp. 21–24.
[22] M. J. DiNezza, X.-H. Zhao, S. Liu, A. P. Kirk, and Y.-H. Zhang, Appl. Phys. Lett. **103**, 193901 (2013).
[23] Y. Zhao, X.-H. Zhao, and Y.-H. Zhang, IEEE J. Photovoltaics **7**, 690–694 (2017).
[24] U. Rau, Phys. Rev. B **76**, 085303 (2007).
[25] O. D. Miller, E. Yablonovitch, and S. R. Kurtz, IEEE J. Photovoltaics **2**, 303–311 (2012).
[26] D. Ding, S. R. Johnson, S.-Q. Yu, S.-N. Wu, and Y.-H. Zhang, J. Appl. Phys. **110**, 123104 (2011).
[27] S. Liu, D. Ding, S. R. Johnson, and Y.-H. Zhang, Proc. SPIE **8256**, 82560M (2012).